JOURNAL OF CATALYSIS **144**, 579–596 (1993)

# The Effect of Passivation on the Activity and Structure of Sulfided Hydrotreating Catalysts

S. P. A. LOUWERS,* M. W. J. CRAJÉ,† A. M. VAN DER KRAAN,† C. GEANTET,‡ AND R. PRINS*

**Laboratorium für Technische Chemie, Eidgenössische Technische Hochschule, 8092 Zürich, Switzerland; †Interfacultair Reactor Instituut, Delft University of Technology, Mekelweg 15, 2629 JB Delft, The Netherlands; and ‡Institut de Recherches sur la Catalyse, 69626 Villeurbanne, France*

Received February 24, 1993; revised June 28, 1993

Air exposure (passivation) and subsequent resulfidation caused a substantial increase in the thiophene hydrodesulfurization activity of sulfided Co–Mo/$Al_2O_3$ catalysts. Since no effect was observed for Mo/$Al_2O_3$ and Co/$Al_2O_3$ catalysts, the passivation effect must be related to the Co–Mo–S structure. EXAFS, Mössbauer emission spectroscopy, and transmission electron microscopy measurements showed that the passivation effect is neither related to a change in the $MoS_2$ dispersion, nor to a change in number and nature of the Co sites. A Co–Mo/$TiO_2$, a Co–Mo/C, and a Co–Mo/$Al_2O_3$ catalyst, which was prepared with the aid of nitrilotriacetic acid, hardly showed an increase in the catalytic activity after passivation. Because of this, and since the Mo–S coordination number for a Co–Mo/$Al_2O_3$ catalyst is increased by passivation, it is concluded that the activity increase originates from a decrease in Mo–support interactions. These interactions are broken when Co atoms migrate to Mo–O–Al bonds during a passivation and resulfidation treatment and assist in the sulfidation of these bonds. Removal of steric hindrance is held responsible for the activity increase. The effect of passivation on the catalytic activity decreased with increasing Co/Mo ratio, probably because at high Co loadings most Mo–O–Al bonds are already sulfided in the first sulfidation step. A maximum activity increase was obtained at a passivation temperature of 340 K. At lower temperatures the oxidation and migration of Co is too slow, whereas at higher temperatures new Mo–O–Al bonds are formed in the passivation treatment. Ni–Mo/$Al_2O_3$ catalysts showed the same behavior as Co–Mo/$Al_2O_3$ catalysts.

## INTRODUCTION

Lower legislative limits on sulfur and nitrogen levels in gasoil are placing higher demands on hydrotreating catalysts and as a result much research is being focused on improving the activity of such catalysts. Thus, catalyst modifiers such as phosphate and fluoride have been found to enhance the activity for hydrodesulfurization (HDS) and hydrodenitrogenation (HDN) of Co–Mo and Ni–Mo catalysts (*1–4*). Coimpregnation of Mo and Co precursors with a nitrogen-containing organic ligand such as nitrilotriacetic acid (NTA) (*5*) increases the activity of the resulting Co–Mo catalyst approximately twofold compared to a catalyst made in a classical two-step impregnation (*6*). Conflicting results have been reported for the influence of calcination temperature on catalyst activity. Increased (*7*) as well as decreased activity (*8*) has been reported. An increase in the sulfidation temperature resulted in an increase of the HDS activity for Co–Mo catalysts supported on $\eta$-$Al_2O_3$ (*9, 10*) and $\gamma$-$Al_2O_3$ (*11*).

An interesting method for improving the catalytic activity was found by Kolboe and Amberg (*12*). When these authors introduced a pulse of oxygen into the thiophene/$H_2$ feed, the activity of an unsupported $MoS_2$ catalyst immediately increased by a factor of 2. However, the effect was only transient, and after a certain time the activity dropped to the same level as before $O_2$ exposure. Electronic influences were sug-

0021-9517/93 $5.00

gested to be responsible for the activity increase. De Beer *et al.* observed the same behavior for supported sulfided Mo/$Al_2O_3$ catalysts (*13*). After exposure to air at room temperature the initial activity increased, but after several minutes time-on-stream it returned to approximately the same level as before air exposure. In contrast, a Co-promoted catalyst displayed a completely different behavior. When exposed to air at room temperature, the activity was significantly increased and did not fall back to the level before air exposure. Furthermore, the activity could be increased again by a second air exposure, and exposing the catalyst to air a third time caused another significant activity enhancement, although the increases became smaller with every subsequent air exposure treatment. De Beer *et al.* (*13*) suggested that the $O_2$ in the air led to a breaking up of the $MoS_2$ crystallites on the alumina support and to additional active sites on the new $MoS_2$ edges. In the unpromoted catalyst these crystallites would grow together again, but in the presence of a Co promoter this would not be possible, because the Co atoms would occupy sites on the new $MoS_2$ edges and prevent the $MoS_2$ particles from sintering together again. Also, Massoth *et al.* investigated the effect of air exposure on the activity of HDS catalysts (*14*). They exposed several sulfided Mo/$Al_2O_3$ catalysts with different Mo loadings to air, and observed that after resulfidation there was a small decrease of the catalytic activity for thiophene hydrodesulfurization. However, the amount of chemisorbed NO had decreased more strongly, suggesting a decrease in the number of active sites and an increase in their intrinsic activity.

To explore further the scope of the passivation effect in hydrodesulfurization and to understand its origin, we have studied several hydrotreating catalysts by catalytic as well as physicochemical methods. The main body of our results and conclusions are presented here, while some preliminary results have been published before (*15*).

## EXPERIMENTAL

### *Catalyst Preparation*

A number of Co- and Ni-promoted and unpromoted Mo catalysts were prepared. First, a series of alumina-supported Co–Mo catalysts with varying Co/Mo atomic ratio, as well as a Ni–Mo/$Al_2O_3$ catalyst, were prepared by pore-volume impregnation of $\gamma$-$Al_2O_3$ (Condea Chemie, 233 $m^2\ g^{-1}$) with aqueous solutions of $(NH_4)_6Mo_7O_{24} \cdot 4H_2O$ (Merck p.a.) and $Co(NO_3)_2 \cdot 6H_2O$ (Johnson Matthey, A.R.) or $Ni(NO_3)_2 \cdot 6H_2O$ (Fluka, purum). After each impregnation the catalysts were dried (12 h, 393 K), heated at 5 K/min to 673 K, and calcined (2 h, 673 K). These catalysts are denoted Co–Mo($x$)/$Al_2O_3$ and Ni–Mo($x$)/$Al_2O_3$, respectively, where $x$ denotes the M/Mo atomic ratio. Analogously, a $^{57}$Co–Mo/$Al_2O_3$ and a Co–Mo/$TiO_2$ catalyst were made with a Co/Mo ratio of 0.3. The $^{57}$Co nitrate solution was obtained from Isotope Products Laboratories, and the $TiO_2$ support was Eurotitania-1 (0.5 $cm^3\ g^{-1}$, 46 $m^2\ g^{-1}$, 99% anatase). An unpromoted Mo/$Al_2O_3$ catalyst was prepared by impregnation with $(NH_4)_6Mo_7O_{24} \cdot 4H_2O$ only. Finally, a Co/$Al_2O_3$ catalyst was made by omitting the Mo impregnation step. The last two catalysts are denoted Mo/$Al_2O_3$ and Co/$Al_2O_3$, respectively. A Co–Mo and a Ni–Mo catalyst with $x = 0.3$ were made according to the method described by van Veen *et al.* (*5*), in which nitrilotriacetic acid (NTA) is used as a complexing agent. These catalysts are denoted Co–Mo(NTA)/$Al_2O_3$ and Ni–Mo(NTA)/$Al_2O_3$.

Carbon-supported catalysts were made by a two-step pore-volume impregnation of a Lonza high surface area graphite (Lonza HSAG-300, 300 $m^2\ g^{-1}$) or a Norit activated carbon (Norit RX3-extra, 1190 $m^2\ g^{-1}$) support. In the first step an aqueous solution of $(NH_4)_6Mo_7O_{24} \cdot 4H_2O$ was employed and in the second step an aqueous solution of $Co(NO_3)_2 \cdot 6H_2O$ or $Ni(NO_3)_2 \cdot 6H_2O$ was used. After each step the catalysts were dried (12 h, 393 K) but not calcined. The

TABLE 1

Catalyst Composition and Notation

| Catalyst | Support | % Mo | % Co(Ni) | M/Mo | Notation |
|---|---|---|---|---|---|
| Mo | $Al_2O_3$ | 7.41 | 0 | 0 | Mo/$Al_2O_3$ |
| Co–Mo | $Al_2O_3$ | 6.82 | 0.42 | 0.10 | Co–Mo(0.1)/$Al_2O_3$ |
| Co–Mo | $Al_2O_3$ | 6.82 | 1.25 | 0.30 | Co–Mo(0.3)/$Al_2O_3$ |
| Co–Mo | $Al_2O_3$ | 6.82 | 1.89 | 0.45 | Co–Mo(0.45)/$Al_2O_3$ |
| Co–Mo | $Al_2O_3$ | 6.82 | 2.51 | 0.60 | Co–Mo(0.6)/$Al_2O_3$ |
| Co–Mo | $Al_2O_3$ | 6.82 | 3.35 | 0.80 | Co–Mo(0.8)/$Al_2O_3$ |
| Co–Mo | $Al_2O_3$ | 6.82 | 4.20 | 1.0 | Co–Mo(1.0)/$Al_2O_3$ |
| Co | $Al_2O_3$ | 0 | 4.50 | | Co/$Al_2O_3$ |
| Co | C(Norit) | 0 | 0.99 | | Co/C(Norit) |
| Co–Mo | $Al_2O_3$ | 7.31 | 1.35 | 0.30 | Co–Mo(NTA)/$Al_2O_3$ |
| Co–Mo | $TiO_2$ | 2.41 | 0.45 | 0.30 | Co–Mo/$TiO_2$ |
| Co–Mo | C(Norit) | 0.49 | 0.089 | 0.30 | Co–Mo/C(Norit) |
| Co–Mo | C(Lonza) | 4.33 | 0.80 | 0.30 | Co–Mo/C(Lonza) |
| Ni–Mo | $Al_2O_3$ | 6.82 | 1.25 | 0.30 | Ni–Mo/$Al_2O_3$ |
| Ni–Mo | $Al_2O_3$ | 3.31 | 0.61 | 0.30 | Ni–Mo(NTA)/$Al_2O_3$ |
| Ni–Mo | C(Norit) | 0.49 | 0.090 | 0.30 | Ni–Mo/C(Norit) |
| $^{57}$Co–Mo | $Al_2O_3$ | 6.82 | 1.26 | 0.30 | $^{57}$Co–Mo(0.3)/$Al_2O_3$ |

Co/Mo and Ni/Mo atomic ratio was 0.3 in all cases. The catalysts are denoted *M*–Mo/C(*s*), where *M* is Co or Ni, and *s* is Norit or Lonza. Additionally, a Co/C(Norit) catalyst was made by impregnation with a $Co(NO_3)_2 \cdot 6H_2O$ solution only. Compositions and notations of all catalysts are given in Table 1. The Mo loading of all $Al_2O_3$-supported catalysts but one was chosen to be around 7%, while the Mo (or Co) loading of the other catalysts was adapted to give a thiophene conversion comparable to that of the Co–Mo(0.3)/$Al_2O_3$ catalyst.

### *Catalytic Activity*

The catalytic activities of the catalysts for thiophene HDS were measured in a microflow reactor at atmospheric pressure. Catalyst samples were sulfided in a flow of 60 $cm^3$ $min^{-1}$ of 10% $H_2S$ in $H_2$. During sulfidation, the temperature was raised at a rate of 6 K $min^{-1}$ to 673 K, except during the first sulfidation of the Co–Mo(NTA)/$Al_2O_3$ catalysts, when the temperature was raised at the much lower rate of 1 K $min^{-1}$, to avoid too early decomposition of the Co–Mo–NTA complex. The temperature was kept at 673 K for 2 h. Next, a gas mixture consisting of 3% thiophene in $H_2$ was introduced into the reactor at a flow rate of 60 $cm^3$ $min^{-1}$. Reaction products were analysed by on-line gas chromatography. The activity of the catalyst samples was expressed as $k_{HDS}$, a first-order rate constant.

After several hours of reaction the catalyst samples were cooled to room temperature under a flow of He, the reactor was opened and the catalyst was exposed to air for a predetermined period (passivation). After passivation, the reactor was closed, the catalyst resulfided, and its activity remeasured as described above. In some cases the catalyst was not cooled to room temperature, but to a predefined temperature between 673 K and room temperature, after which it was not exposed to air, but to a flow of 5% $O_2$/He, and the catalyst was left overnight under this flowing mixture.

### *EXAFS*

The Co and Mo EXAFS of the Co–Mo(0.3)/$Al_2O_3$ catalyst have been measured after the first sulfidation, after a passivation treatment of 1 week, and finally after a subsequent resulfidation. The Co and Mo EXAFS were measured on beamlines 7.1 and 9.3, respectively, of the synchrotron radiation source (SRS) in Daresbury, United Kingdom. The Mo EXAFS of the sample after the first sulfidation has been measured on beamline 9.2 as well. The pretreatment and the X-ray absorption measurement of the samples (*15*), as well as the measurements of the reference compounds (*16*), were described before. For the Co–S, Co–Mo, and Co–Co contributions the reference compounds mentioned in Ref. (*17*) were used, while the references used for the Mo–Mo, Mo–S, and Mo–Co contributions are mentioned in Ref. (*18*). In addition the Ni–O coordination in Ni–O was used for the Co–O coordination (*19*).

### *Mössbauer Emission Spectroscopy (MES)*

To study how passivation influences the Co environment, the MES spectrum of the $^{57}$Co–Mo(0.3)/$Al_2O_3$ catalyst was recorded after several pretreatments. Sulfidation and resulfidation treatments were carried out in an *in situ* Mössbauer reactor (*20*), according to the same procedure as for the EXAFS measurements. Passivation was done by exposing the catalyst to ambient air at room temperature. The MES experiments were carried out as described in Ref. (*21*).

### *Transmission Electron Microscopy*

High-resolution transmission electron microscopy (HRTEM) measurements of the Co–Mo(0.3)/$Al_2O_3$ catalyst after sulfidation, after sulfidation and a subsequent reaction, as well as after six reaction–passivation–resulfidation cycles were performed on a JEOL 100 CX microscope. The catalyst particles were ultrasonically dispersed on a copper grid coated with a thin carbon film (<10 nm).

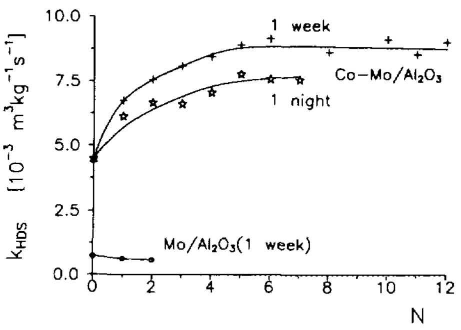

FIG. 1. Steady-state HDS rate constants (after 300 min reaction time) as a function of the number of passivation cycles *N* (and indicated passivation time) for the Co–Mo(0.3)/$Al_2O_3$ and Mo/$Al_2O_3$ catalysts.

## RESULTS

### *Catalytic Activity*

Several passivation cycles with subsequent resulfidation and activity measurement were applied to the Co–Mo(0.3)/$Al_2O_3$ and Mo/$Al_2O_3$ catalysts. The resulting steady-state rate constants $k_{HDS}$ (at 300 min reaction time) are plotted in Fig. 1 as a function of *N*, the number of passivation cycles. For the Co–Mo(0.3)/$Al_2O_3$ catalyst two series of experiments were performed, one in which a passivation time of 1 night was applied, and one in which this time was extended to 1 week. The unpromoted Mo/$Al_2O_3$ catalyst reacted very slowly and therefore only the results with a passivation time of 1 week are presented. As seen from Fig. 1, passivation increases the activity of the Co-promoted catalyst, but does not increase the steady-state activity of the unpromoted catalyst. In addition, the effect of 1 week air exposure is significantly higher than that of 1 night exposure.

To see whether the activity increase of the promoted catalyst is caused by the passivation treatment proper or by the resulfidation treatment, we subjected the Co–Mo(0.3)/$Al_2O_3$ catalyst to several cycles of sulfidation and activity measure-

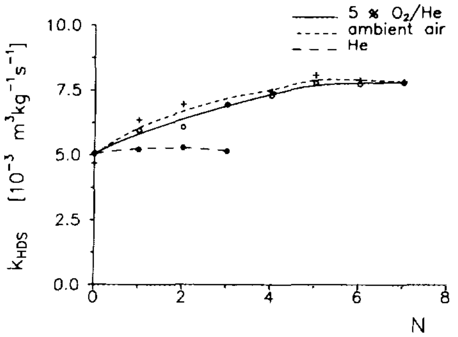

FIG. 2. Steady-state HDS rate constants as a function of the number of passivation cycles $N$ for the Co–Mo(0.3)/$Al_2O_3$ catalyst after passivation during one night in helium, ambient air, or 5% $O_2$/He.

ments. After each cycle the catalyst was cooled to room temperature under flowing He, left overnight under flowing He, and resulfided. A comparison of the results of these experiments with those of passivation (1 night)–resulfidation cycles on the same catalyst showed clearly (Fig. 2) that the resulfidation procedure itself does not produce a more active catalyst, and that exposure to air is necessary to observe an activity increase. To prove that oxygen, and not water vapor, $CO_2$ or other components in the air, causes the passivation effect we carried out two series of experiments with the Co–Mo(0.3)/$Al_2O_3$ catalyst. In one series this catalyst underwent a number of passivation cycles (with subsequent activity measurements) in ambient air, whereas in the other series the catalyst was exposed to a flow of 5% $O_2$/He. The results of the two series were identical; ambient air had the same effect on the activity as the 5% $O_2$/He gas mixture (cf. Fig. 2).

Finally, we checked whether exposure to air with subsequent sulfidation alone results in an activity increase, or whether the thiophene hydrodesulfurization reaction and the reaction products play a role. For example, carbon residues formed during the reaction might influence the active sites during the passivation and resulfidation. Therefore, the catalytic activity of the Co–Mo(0.3)/$Al_2O_3$ catalyst was measured after a first sulfidation, and after a subsequent passivation (1 week) and resulfidation. The steady-state reaction rate after the first sulfidation was 4.5 $m^3$ $kg^{-1}$ $s^{-1}$, whereas after the resulfidation it was 7.1 $m^3$ $kg^{-1}$ $s^{-1}$. When the same catalyst was not subjected to an activity measurement after sulfidation, but directly to a passivation and resulfidation, the steady-state reaction rate was 7.6 $m^3$ $kg^{-1}$ $s^{-1}$. Thus, without reaction there is an even larger effect on the activity, which might be due to the absence of coke formed during the first activity measurement. On the other hand, the uncertainty in the activity measurement is about 5% and therefore not much weight can be placed on the difference between the values of 7.1 and 7.6 $m^3$ $kg^{-1}$ $s^{-1}$.

The influence of the Co/Mo atomic ratio on the passivation effect was studied on a series of alumina-supported Co–Mo catalysts with Co/Mo atomic ratios between 0 and 1.0, and a passivation time of 1 week. The results are presented in Fig. 3. The ratios of the steady state rate constants after the last passivation cycle ($k_{HDS,end}$) and the initial rate constants before the first passivation ($k_{HDS,0}$), are given in Table 2. This ratio is a measure of the effect of passivation on the activity. It is highest for Co/Mo = 0.1, and decreases with increasing Co/Mo ratio, showing that the maximum benefit is obtained for catalysts with a small amount of

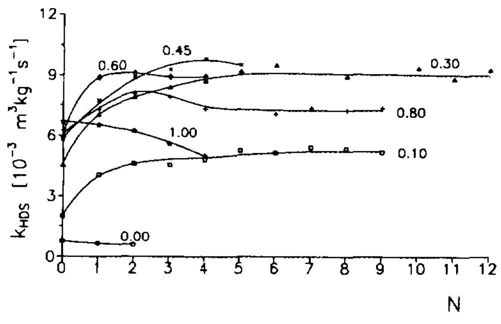

FIG. 3. Steady-state HDS rate constants as a function of the number of passivation cycles $N$ (1 week passivation) for Co–Mo/$Al_2O_3$ catalysts with different Co/Mo atomic ratios.

TABLE 2

Ratio of the HDS Rate Constant after the Last Passivation ($k_{HDS,end}$) and before the First Passivation ($k_{HDS,0}$)

| Catalyst | $k_{HDS,end}/k_{HDS,0}$ |
|---|---|
| $Mo/Al_2O_3$ | 0.8 |
| $Co-Mo(0.1)/Al_2O_3$ | 2.6 |
| $Co-Mo(0.3)/Al_2O_3$ | 2.1 |
| $Co-Mo(0.45)/Al_2O_3$ | 1.7 |
| $Co-Mo(0.6)/Al_2O_3$ | 1.5 |
| $Co-Mo(0.8)/Al_2O_3$ | 1.2 |
| $Co-Mo(1.0)/Al_2O_3$ | 0.8[a] |

[a] The activity had not yet reached a constant value after the last passivation, and was still decreasing.

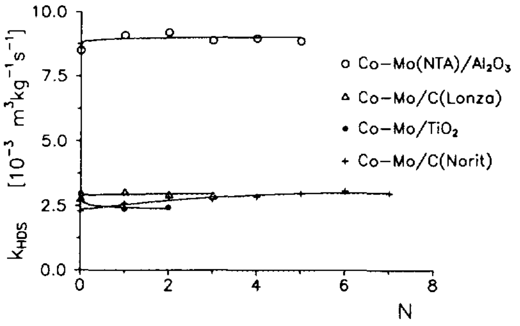

FIG. 5. Steady-state HDS rate constants as a function of the number of passivation cycles $N$ (1 night each) for the $Co-Mo(NTA)/Al_2O_3$, Co–Mo/C(Norit), $Co-Mo/TiO_2$, and Co–Mo/C(Lonza) catalysts.

Co. For the $Co-Mo(1.0)/Al_2O_3$ catalyst with the highest Co/Mo ratio, a negative effect of passivation is observed: the catalytic activity decreases every time the catalyst is passivated (Fig. 3). In Fig. 4 the initial catalytic activities (before the first passivation) and the activities after one, two, and four passivation cycles are presented as a function of the Co/Mo ratio. The initial catalytic activity steadily increases within the range of Co/Mo ratios studied, and up to a Co/Mo atomic ratio of 0.3 the activity seems to increase linearly with the Co/Mo ratio. The catalytic activity of the passivated (and resulfided) catalysts goes through a maximum with increasing Co/Mo ratio. This maximum shifts to a lower Co/Mo ratio when more passivation cycles are applied.

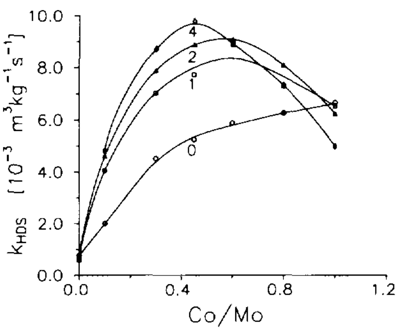

FIG. 4. Steady-state HDS rate constants of $Co-Mo/Al_2O_3$ catalysts as a function of the Co/Mo atomic ratio and the number of passivation cycles.

Co–Mo catalysts on supports other than $\gamma-Al_2O_3$ ($Co-Mo/TiO_2$, Co–Mo/C(Norit), Co–Mo/C(Lonza)), or prepared by the NTA recipe ($Co-Mo(NTA)/Al_2O_3$), did not show much increase in activity (Fig. 5). The $Co/Al_2O_3$ and Co/C(Norit) catalysts did not show an increase in activity either. On the contrary, their activities decreased by passivation.

The influence of the passivation temperature was investigated for the $Co-Mo(0.3)/Al_2O_3$ catalyst in experiments in which the catalyst was passivated by a flow of 5% $O_2/He$ overnight. The passivation temperature was varied between room temperature and 673 K. In Fig. 6 the steady-state activities after five passivation cycles are given as a function of the passivation temperature. It can be seen that at every passivation temperature the activity is higher than before passivation, but that a maximum is obtained at 323 K.

Finally, the effect of passivation on the activity of three Ni–Mo catalysts ($Ni-Mo/Al_2O_3$, $Ni-Mo(NTA)/Al_2O_3$, and Ni–Mo/C(Norit)) was studied. It was found that the time of passivation was important for these catalysts. For the $Ni-Mo/Al_2O_3$ catalyst no significant activity increase was seen after overnight passivation, in contrast to the

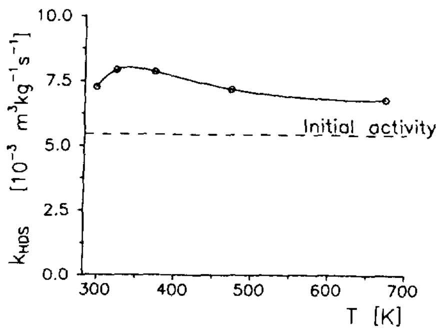

FIG. 6. Steady-state HDS rate constants for the Co–Mo(0.3)/$Al_2O_3$ catalyst after five passivation cycles (1 night each) as a function of the passivation temperature.

Co–Mo(0.3)/$Al_2O_3$ catalyst, where the activity had already gone up by more than 30% (Fig. 1). However, after a passivation time of 3 days the Ni–Mo/$Al_2O_3$ catalyst showed an activity increase as well (Fig. 7), although not as large as the Co–Mo(0.3)/$Al_2O_3$ catalyst. After seven 3-day passivation cycles the activity increase for the Ni–Mo(0.3)/$Al_2O_3$ catalyst is approximately the same as that after seven 1-night passivation cycles of the Co–Mo/$Al_2O_3$ catalyst (ca. 65%), but whereas the activity of the Co–Mo(0.3)/$Al_2O_3$ catalyst seems to level off after seven passivation cycles, the Ni–Mo/$Al_2O_3$ catalyst has not reached a constant value yet. These results indicate that the effect of passivation is slower for Ni–Mo/$Al_2O_3$ catalysts (it takes more cycles and/or a longer passivation time before a comparable effect is seen), but eventually a larger increase is obtained for the Ni–Mo/$Al_2O_3$ catalyst. The effect of passivation (passivation time 3 days) on the activity of the Ni–Mo(NTA)/$Al_2O_3$ and the Ni–Mo/C(Norit) catalysts is much smaller than that for the Ni–Mo/$Al_2O_3$ catalyst. However, some increase can be seen (Fig. 7).

## *EXAFS*

*Co EXAFS.* The EXAFS functions for the Co–Mo(0.3)/$Al_2O_3$ catalyst after sulfidation (S), passivation for 1 week (SO), and resulfidation (SOS) have been obtained from the X-ray absorption data as described before (*16*). The *k* and *R* ranges used are given in Table 3 and the resulting structural parameters are given in Table 4. A comparison between the experimental data and the calculated spectra has already been published (*15*). The data show that in the sulfided state (the S and SOS catalysts) the Co-atoms are surrounded by six sulfur atoms, at two different Co–S distances. Four sulfur atoms are at 2.20 Å, and two at a somewhat longer atomic distance of 2.26 Å. We checked whether a Co–Co contribution at 2.50 Å, representative of $Co_9S_8$, was present. Although it was possible to fit the spectra with this contribution, together with a Co–S contribution at 2.22 Å and a Co–Mo contribution at 2.87 Å, we reject this possibility since

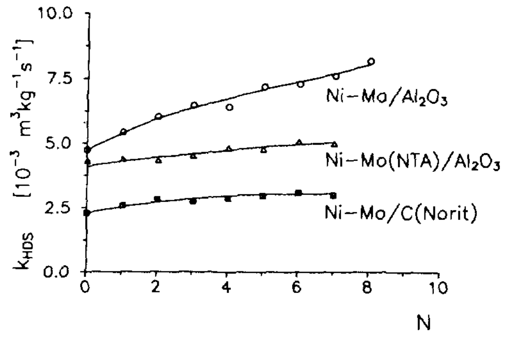

FIG. 7. Steady-state HDS rate constants as a function of the number of passivation cycles *N* for the Ni–Mo catalysts. The passivation time per cycle was 3 days.

TABLE 3

Ranges in *k*- and *R*-Space Used in the Analyses of the EXAFS Spectra of the Co–Mo(0.3)/$Al_2O_3$ Catalyst after the First Sulfidation (S), after a Subsequent Passivation Treatment of 1 Week (SO), and after the Second Sulfidation (SOS)

| Catalyst | Co EXAFS | | Mo EXAFS | |
|---|---|---|---|---|
| | *k* Range ($Å^{-1}$) | *R* Range (Å) | *k* Range ($Å^{-1}$) | *R* Range (Å) |
| S | 2.65–11.53 | 0.68–3.08 | 3.16–14.15 | 1.04–3.54 |
| SO | 1.95–11.61 | 0.58–2.92 | 3.20–13.49 | 1.24–3.60 |
| SOS | 2.70–11.53 | 0.66–3.15 | 3.12–14.13 | 1.04–3.54 |

TABLE 4

Structural Parameters of the Co–O, Co–S, and Co–Mo Coordinations for the Co–Mo(0.3)/$Al_2O_3$ Catalyst

| Catalyst | $N$ | $\Delta\sigma^2$ (Å$^2$) | $R$ (Å) | $E_0$ (eV) | $N$ | $\Delta\sigma^2$ (Å$^2$) | $R$ (Å) | $E_0$ (eV) |
|---|---|---|---|---|---|---|---|---|
| | Co–O coordination | | | | First Co–S coordination | | | |
| S | | | | | 4.4 | 0.0058 | 2.20 | 4.9 |
| SO | 4.0 | 0.0060 | 2.01 | 4.9 | 2.1 | −0.0003 | 2.22 | 7.1 |
| SOS | | | | | 4.5 | 0.0054 | 2.20 | 4.1 |
| | Second Co–S coordination | | | | Co–Mo coordination | | | |
| S | 1.8 | 0.0020 | 2.26 | −9.4 | 0.9 | 0.0050 | 2.86 | −10.2 |
| SO | | | | | 0.3 | −0.0003 | 2.80 | 4.7 |
| SOS | 1.5 | −0.0004 | 2.25 | −9.4 | 1.0 | 0.0056 | 2.85 | −11.5 |

*Note*. The coordination numbers have been corrected for the photoelectron mean free path (λ) dependence, assuming that λ = 5 Å. The coordination number is represented by $N$, the atomic distance by $R$, the difference between the inner potentials of sample and reference compound by $E_0$, and the difference between the Debye–Waller factors of the sample and the reference compound by $\Delta\sigma^2$. S, SO, and SOS as in Table 3.

it did not lead to an improvement of the quality of the fit. Furthermore the Co–S coordination number in this fit was about 6. If substantial amounts of $Co_9S_8$ (in which most of the Co atoms are surrounded by four sulfur atoms) would have been present, this should have shown up in a lowering of the Co–S coordination number, since EXAFS is a bulk technique and detected coordination numbers are averaged over all Co atoms present in the sample.

In the passivated state the Co atoms are partly oxidized as is apparent from the appearance of a Co–O contribution and the loss of sulfur and molybdenum neighbors. Also in other studies an oxidation of Co after exposure to air has been observed (*6*, *22–24*). The data furthermore show that the Co environments in the sulfided (S) and the resulfided (SOS) catalyst are practically identical. These results are supported by the XANES spectra (Fig. 8). Also here no difference between the S and SOS catalysts can be seen. The large white line for catalyst SO again indicates oxidation of Co, since oxidic Co is more ionic than sulfidic Co, and the intensity of the white line is related to the ionicity (*25*). The pre-edge peak is small for all catalysts, which suggests that most of the Co is not tetrahedrally surrounded by sulfur (*17*).

*Mo EXAFS*. The EXAFS functions have been calculated from the Mo *K*-edge X-ray absorption data using the same procedure as for the Co EXAFS. Also the fitting procedure of the EXAFS spectrum of catalyst S measured on beamline 9.2 was done in a similar way. It turned out that the EXAFS spectra of this catalyst measured on beamlines 9.2 and 9.3 showed substantial differences: the amplitudes of the EXAFS functions of samples measured on beamline 9.3 were significantly lower than those for samples measured on beamline 9.2. Since our reference compounds were measured on beamline 9.2, it was not possible to use their spectra to fit the EXAFS spectra of the SO and SOS catalysts, which were measured on beamline 9.3. Therefore the EXAFS spectrum of the S catalyst which was measured on both beamlines was used as a secondary reference. The Mo–S, Mo–Co, and Mo–Mo shells of the spectrum of the S catalyst measured on beamline 9.3 were fitted as usual with the references measured at beamline 9.2, and the resulting structural parameters were corrected using the results obtained for this catalyst on beamline 9.2. The corrected Mo–S, Mo–Co, and Mo–Mo contributions were then used as references for the EXAFS spectra of the SO and SOS catalysts. The $k$ and $R$ ranges used to isolate

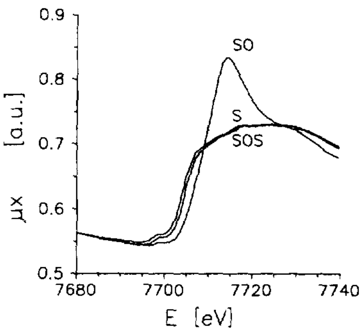

FIG. 8. XANES spectra at the Co *K*-edge for the Co–Mo(0.3)/$Al_2O_3$ catalyst after sulfidation (S), after 1 week passivation (SO), and after passivation and resulfidation (SOS).

TABLE 5

Structural Parameters of the Mo–S and Mo–Mo Coordinations for the Co–Mo(0.3)/$Al_2O_3$ Catalyst

| Catalyst | $N$ | $\Delta\sigma^2$ (Å$^2$) | $R$ (Å) | $E_0$ (eV) | $N$ | $\Delta\sigma^2$ (Å$^2$) | $R$ (Å) | $E_0$ (eV) |
|---|---|---|---|---|---|---|---|---|
| | Mo–S coordination | | | | Mo–Mo coordination | | | |
| S | 5.4 | 0.0019 | 2.41 | 1.9 | 2.9 | 0.0026 | 3.15 | 1.4 |
| SO | 4.8 | 0.0015 | 2.42 | 1.3 | 2.3 | 0.0021 | 3.13 | 4.6 |
| SOS | 6.6 | 0.0017 | 2.41 | 1.2 | 3.2 | 0.0012 | 3.15 | 2.5 |

*Note*. The coordination numbers have been corrected for the photoelectron mean free path ($\lambda$) dependence, assuming that $\lambda = 5$ Å. $N$, $R$, $E_0$, $\Delta\sigma^2$, S, SO, and SOS are as in Table 4.

contributions of interest are given in Table 3. The results of the analyses are given in Table 5, and a comparison between experimental data and fits is given in Fig. 9.

The results show that all three catalysts have $MoS_2$-like Mo–S and Mo–Mo atomic distances, showing that the Mo is mainly in a $MoS_2$ structure. In addition a Mo–Co coordination is seen. The uncertainties in the structural parameters for this contribution are, however, large, since the small Mo–Co contribution is situated between the two much bigger Mo–S and Mo–Mo contributions. Also the use of the Mo–Co contribution of catalyst S as a reference for the SO and SOS catalysts increases the inaccuracy for the Mo–Co contribution in the last two catalysts to a large extent, and structural parameters cannot be determined reliably. Therefore, the parameters for this contribution have been omitted from Table 5. Information about the Co–Mo coordination should be derived from the Co EXAFS, and not from the Mo EXAFS. The Mo–S and Mo–Mo coordinations can be determined much better, though, and a comparison of the S and SOS catalysts indicates that the passivation-resulfidation leads to an increase in the Mo–S and Mo–Mo coordination numbers.

The Mo–S coordination number of catalyst SO is lower than for catalyst S, suggesting that oxidation of Mo had taken place. Other authors also observed oxidation of Mo after prolonged exposure to air (*22, 26–28*), although short exposure times

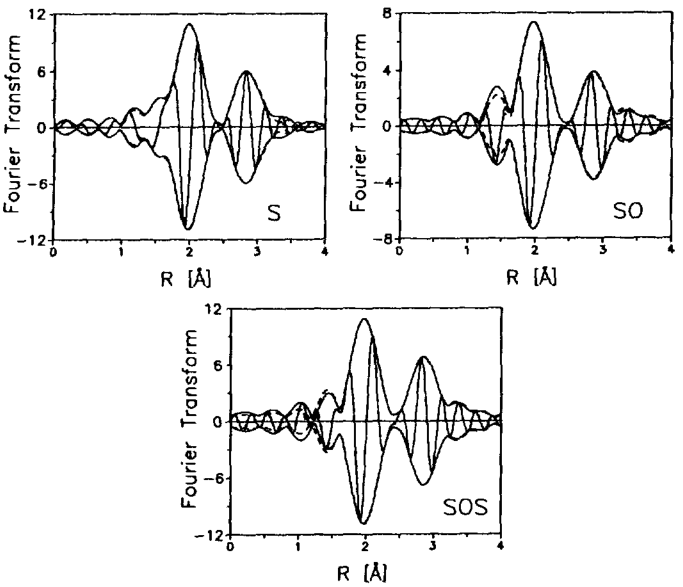

FIG. 9. Comparison of the $k^3$ Fourier-transformed Mo EXAFS data of the Co–Mo(0.3)/$Al_2O_3$ catalyst (drawn lines) and the corresponding calculated Fourier transforms (interrupted lines) after sulfidation (S), subsequent passivation (SO), and resulfidation (SOS).

hardly affected Mo (*26, 28–30*). The Mo–Mo coordination number is suspiciously low for the SO catalyst, since it is not very likely that the $MoS_2$ structure can be retained for $N_{Mo-Mo} = 2.3$. In that case additional atomic distances would be expected. It might be that disorder is responsible for the low Mo–Mo coordination number (*31*), or that some of the sulfur neighbors have been replaced by oxygen neighbors. Since oxidation of Mo should lead to a Mo–O contribution in the Mo EXAFS, we tried to fit the spectrum of the passivated catalyst by including a Mo–O contribution. The quality of the fit improved by the addition of this coordination, but the improvement was not large enough to be able to conclude unequivocally that a Mo–O coordination is present. Because of this we refrain from presenting a Mo–O coordination number and distance. The difficulty to detect Mo–O bonds is a weakness inherent to the EXAFS technique. For example, the EXAFS determination of the Mo–O coordination number of $MoO_3$ systematically gives a much lower value than the crystallographic value of 6 (*32, 33*). This is because in structures with several unequal metal-oxygen distances the beating between their EXAFS contributions reduces the overall EXAFS intensity markedly in the $k$ = 3–8 $Å^{-1}$ range in which oxygen neighbors can be measured and analysed. An attempt to detect Mo–O contributions in the XANES region also failed, since the XANES spectra of all three S, SO, and SOS samples looked very much alike. Analogously, Chiu *et al.* observed that the $1s \rightarrow 4d$ shoulder of $MoO_3$ was masked by the dominant leading edge of $MoS_2$ in a 1 : 2 physical mixture of $MoO_3$ and $MoS_2$ (*34*).

### *Mössbauer Emission Spectroscopy*

Figure 10 shows the MES spectra of the $^{57}Co-Mo(0.3)/Al_2O_3$ catalyst after different pretreatments. The spectrum of the sulfided catalyst contains a doublet with a quadrupole splitting of 0.86 mm $s^{-1}$, which indicates that most of the Co is sulfided. This quadrupole splitting is somewhat small for a catalyst containing Co mainly in the CoMoS structure and not in $Co_9S_8$. It has previously been reported that a quadrupole splitting in the range 1.0–1.3 mm $s^{-1}$ is indicative for CoMoS (*35*). The value of 0.86 indicates that the formed Co-sulfide species are not optimally dispersed.

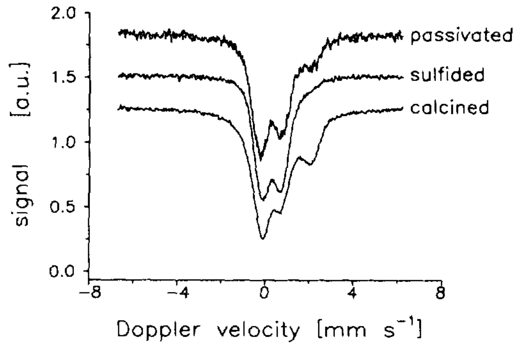

FIG. 10. Mössbauer emission spectra of the $^{57}Co-Mo(0.3)/Al_2O_3$ catalyst after calcination, after the first sulfidation, and after the first passivation (for 6 days).

The spectra of the catalysts after passivation were fitted with two doublets, one with an isomer shift of 0.21 mm $s^{-1}$ and a quadrupole splitting between 1.00 and 1.04 mm $s^{-1}$, typical for the CoMoS structure. The occurrence of this doublet indicates that, although substantial oxidation of Co has taken place, some Co atoms are still present in a (not oxidised) CoMoS structure. This was also observed by Crajé *et al.* (*36*), who found that exposing a Co–Mo/C catalyst with a very low Co/Mo atomic ratio of 0.0095 to air for 23 days did not result in any changes of the MES spectrum. The other doublet has an isomer shift of 1.03 mm $s^{-1}$ and a quadrupole splitting between 2.0 and 2.1 mm $s^{-1}$, pointing to the presence of high-spin $Co^{2+}$ ions. This shows that part of the Co is oxidized after passivation. Co is not completely oxidized, however, since this doublet is less intense than that of the calcined catalyst. The contribution of the high-spin $Co^{2+}$ ions to the spectrum gradually increased from 12% after a passivation time

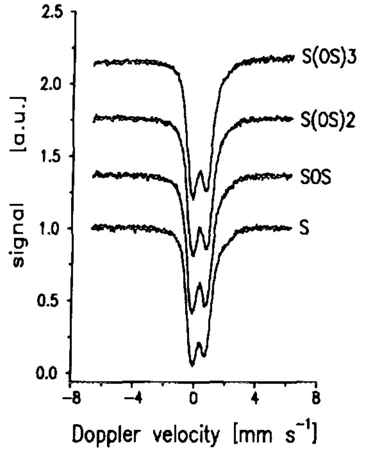

FIG. 11. Mössbauer emission spectra of the $^{57}$Co-Mo(0.3)/$Al_2O_3$ catalyst in the sulfided state after several passivation cycles.

of 1 day to 16% after 1 week of air exposure, indicating that Co is slowly oxidized. The same phenomenon can be seen during the third passivation, where the contribution of the high-spin $Co^{2+}$ to the spectrum increases from 7% after 1 day to 13% after 1 week air exposure. It must be realized that these percentages do not directly represent the amount of oxidic or sulfidic Co, since the sensitivity for the two kinds of Co can be quite different in MES. The sensitivities depend on Debye temperatures and are temperature dependent. Therefore, one has to look at the trend, rather than at the absolute numbers.

The MES spectra of the S, SOS, S(OS)2 and S(OS)3 catalysts are compared in Fig. 11. These spectra were fitted with one doublet only, since the fits with more than one doublet could not be rationalized. The spectrum changed somewhat after the first passivation and resulfidation, as is indicated by an increase in the quadrupole splitting from 0.86 to 0.92 mm s$^{-1}$. After the first passivation cycle no more changes were observed, the spectra of the SOS, S(OS)2, and S(OS)3 catalysts being identical. Finally, MES measurements on the $^{57}$Co-Mo(0.3)/$Al_2O_3$ catalyst were done after the first, second, third and fourth passivation (passivation time 1 week). No substantial differences were found.

### *Transmission Electron Microscopy*

The results of the transmission electron microscopy measurements on the Co-Mo(0.3)/$Al_2O_3$ catalyst after three different treatments are given in Fig. 12. The S catalyst had undergone one sulfidation, while the (S + R) catalyst had undergone an additional thiophene HDS reaction. Electron micrographs were also made after six reaction–passivation–resulfidation cycles with 1 week passivation each (the S(ROS)6R catalyst). Before each passivation, as well as after the last passivation, the catalyst had been sulfided and an HDS reaction had been performed. After six passivation cycles the catalyst reached its maximum activity (see Fig. 1). The S and (S + R) catalysts were transferred to the electron microscope under an $N_2$ atmosphere, and they had never been in contact with oxygen. This was not the case for the S(ROS)6R catalyst. After the seventh reaction this catalyst was transferred to a glove box, where it was kept under a $N_2$ atmosphere until the time of measurement. During the transfer from the reactor to the glove box, however, the catalyst came in contact with air.

The slab length distribution and the stacking distribution are given in Figs. 12a and 12b, respectively. The average $MoS_2$ slab size was 3.1 nm for the S and (S + R) catalysts and 2.8 nm for the S(ROS)6R catalyst. The average stacking numbers were 1.7, 1.6, and 1.5, respectively. Only minor differences are observed. The slab length for the S(ROS)6R catalyst seems somewhat smaller than for the other catalysts, but this might be an artefact, since the edges of the $MoS_2$ slabs do not appear as true lamellar structures, possibly due to oxidation.

## DISCUSSION

### *Origin of the Activity Increase*

The results presented in Figs. 2 and 3 unambiguously show that the activity increase

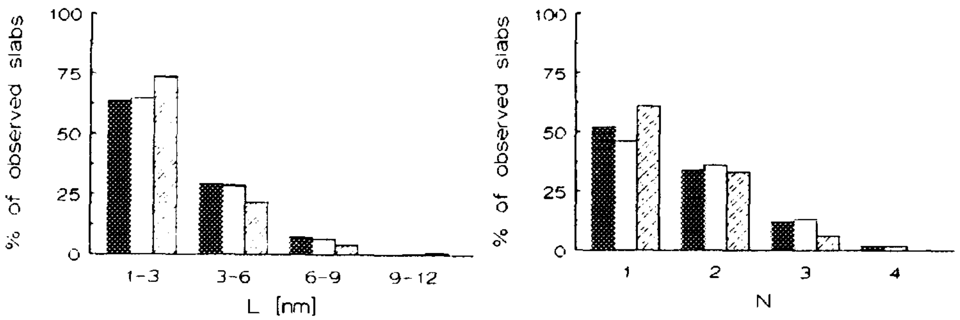

FIG. 12. Distribution of the $MoS_2$ slab length $L$ and stacking number $N$ in the Co–Mo(0.3)/$Al_2O_3$ catalyst after the first sulfidation (black), after a sulfidation with subsequent reaction (white), and after six passivation cycles with subsequent resulfidation and reaction (hatched).

after passivation and resulfidation is solely due to exposure to oxygen. The observation that neither the Co/C(Norit) and Co/$Al_2O_3$ catalysts, nor the Mo/$Al_2O_3$ catalyst show an activity increase upon passivation indicates that the passivation effect is linked to the CoMoS structure. Various explanations can be suggested for the passivation effect. For instance, new, very active sites may be formed. However, these new sites would have to be present in very small amounts, since no evidence for them is found in Co-EXAFS, Mo-EXAFS, or MES. This means that their intrinsic activity must be very high to cause a doubling of the activity. No indication for such new, highly active sites has, however, been found. Another possibility was mentioned by de Beer *et al.* (*13*). They suggested that oxygen breaks up the $MoS_2$ particles during passivation, thus enlarging the $MoS_2$ edge surface and increasing the number of active sites. The role of Co would be to stabilise the higher $MoS_2$ dispersion. However, in a promoted catalyst the most active sites are related to Co. The promoter effect of Co on $MoS_2$ catalysts has, on the one hand, been ascribed to combined Co–Mo sites which are much more active than Mo sites (*37*), or on the other hand to Co atoms as the active sites, $MoS_2$ merely serving as a (secondary) support (*38, 39*). Either way, it means that the distribution of the Co atoms, rather than the $MoS_2$ dispersion, determines the activity. However, EXAFS and MES show that most of the Co atoms are already well dispersed in the CoMoS phase after the first sulfidation. Although the MES spectra of the sulfided and resulfided $^{57}$Co–Mo(0.3)/$Al_2O_3$ catalysts show an increase in the quadrupole splitting upon passivation, which indicates that the cobalt becomes more highly dispersed, the quadrupole splitting does not change any more after the first passivation, whereas the activity still increases. The Co EXAFS data show that after the first sulfidation nearly all Co is already in the CoMoS structure, and that no large increase in the amount of CoMoS is possible. Also, in the plot of $k_{HDS}$ (before the first passivation) vs. the Co/Mo atomic ratio (Fig. 4) no deviation from a straight line is seen up to a Co/Mo ratio of 0.3, and this curve levels off only at higher Co/Mo ratios. When large amounts of $Co_9S_8$ were present, one would expect this curve to level off much sooner. All this shows that the activity increase is not related to a dramatic change in the number of Co atoms in the CoMoS structure.

This leaves a third explanation for the passivation effect, namely, an increase in the activity of the existing sites, either due to an increase in the intrinsic activity, or due to a removal of steric hindrance. Massoth *et al.* concluded that Mo sites on Mo/$Al_2O_3$ catalysts become more active after passivation (*14*). The amount of NO chemisorbed on passivated and resulfided catalysts was found to be lower than that on catalysts not exposed to air, although the overall activity was approximately the same. They therefore suggested that the number of active sites had decreased, but that their intrinsic activity had increased due to the presence of oxygen atoms. The passivated and resulfided $Mo/Al_2O_3$ catalyst was, however, not flushed with helium at 400°C before the NO chemisorption measurement, as the freshly sulfided $Mo/Al_2O_3$ had been. When no helium flushing is applied, there will be less desorption of $H_2S$ from the catalyst surface and as a consequence less NO chemisorption. The thiophene HDS rate constants, on the other hand, were measured after 18 h on stream and thus the influence of a different pretreatment was equalised, explaining why there is not much difference in the rate constants. We therefore believe that the results of Massoth *et al.* do not prove that passivation of a sulfided $Mo/Al_2O_3$ catalyst leads to a higher intrinsic activity. Also, our Mo EXAFS spectra do not show any evidence for a Mo–O contribution after passivation and resulfidation. If anything, the degree of sulfidation is larger, not smaller, as indicated by the increase in the Mo–S coordination number.

Since the structural parameters of the $Co–Mo(0.3)/Al_2O_3$ catalyst after the first sulfidation and after the resulfidation are identical within the limits of accuracy, the structure of the active sites cannot have changed dramatically. Also the XANES spectra show no significant differences. In agreement herewith, the Co structure in the passivated state (which is the precursor for the Co environment after resulfidation) after several passivations does not differ either, since catalyst SO has the same Mössbauer spectrum as the S(OS)O, S(OS)2O, and S(OS)3O catalysts. Therefore, the increase in activity is not related to a change in the local environment of the Co atoms, and thus not to a change in the intrinsic activity.

Whereas the physical EXAFS and MES measurements do not give a direct clue about the origin of the passivation effect, the catalytic activity results obtained with other supports suggest that catalyst–support interactions may play a role. The catalytic activities of the $Co–Mo(NTA)/Al_2O_3$, $Co–Mo/TiO_2$, and Co–Mo/C(Lonza) catalysts (Fig. 5) showed only small increases after successive passivation treatments, while the Co–Mo/C(Norit) catalyst showed a slightly larger increase. The Mo–support interactions in these catalysts are weak. Co–NTA and Mo–NTA complexes are present in the $Co–Mo(NTA)/Al_2O_3$ catalyst during impregnation. This catalyst is not calcined, but directly, gently sulfided with a $H_2S–H_2$ mixture (*5*). After sulfidation the NTA ligands have disappeared (van Veen, private communication), probably due to decomposition to $NH_3$, $CH_4$, and CO. Since the Co and Mo ions in the oxidic precursor state were protected from contact with the support by the NTA ligands, they will be directly transformed into a fully sulfided CoMoS structure, without any Co– or Mo–support bonds. On a $TiO_2$ support the Mo-support interactions are also small, as indicated by the ease with which Mo can be sulfided on this support (*40*). Also on a carbon support the Mo–support interactions are small. Hayden *et al.* (*41*), for example, observed that when Mo oxide supported on $Al_2O_3$ was heated under oxygen a well-dispersed molybdenum oxide phase was formed, while on a carbon support bulk $MoO_3$ was formed. This indicated that the $Mo–Al_2O_3$ interaction is stronger than the Mo–C interaction. Furthermore, Scheffer *et al.* reported that a Mo/C catalyst could be sulfided at much lower temperatures than a $Mo/Al_2O_3$ catalyst (*42*). On graphitic carbon, such as the Lonza carbon used for the Co–Mo/C(Lonza) catalysts, hardly any functional groups are present (*43*), which suggests that on this support in particular the Mo–support interactions can be neglected. Activated carbon, on the other hand, the support in the Co–Mo/C(Norit) catalyst, contains a relatively high percentage of surface oxygen functional groups (*44*), and therefore the Mo–support interactions may be stronger than in the case of a graphitic carbon. However, also on activated carbon the Mo–support interactions are substantially weaker than on $Al_2O_3$, where Mo–support interactions are substantial (*30*, *35*, *41*, *45*).

Thus, there seems to be a correlation between the strength of the Mo–support interactions and the effect of passivation on the catalytic activity. When Mo–support interactions are weak or absent, as in the Co–Mo(NTA)/$Al_2O_3$, Co–Mo/$TiO_2$ and Co–Mo/C(Lonza) catalysts, there is hardly any passivation effect. When the interaction is strong (the Co–Mo(0.3)/$Al_2O_3$ catalyst) there is a large passivation effect, and in the intermediate situation (the Co–Mo/C(Norit) catalyst) there is a small passivation effect. A decreased Mo–support interaction can lead to a higher catalytic activity, as is evident from several studies (*6*, *40–42*, *46–51*), in which high catalytic activities were obtained for catalysts in which Mo interacts only weakly with the support. This correlation between the passivation effect and the Mo–support interactions is substantiated by our Mo EXAFS results. Table 5 shows that the Mo-S coordination number is significantly increased by a passivation and subsequent sulfidation, which indicates a larger degree of sulfidation for the Mo. This takes place without an increase in the $MoS_2$ slab size, since the TEM results do not show any growth of the $MoS_2$ particles. Also the Mo–Mo coordination number hardly changed. The increase in $N_{Mo-S}$, therefore, might be attributed to a replacement of Mo–O bonds (or Mo–O–Al interactions) by Mo–S bonds, which implies a decrease in Mo–support interactions.

Several authors have tried to explain why a lowering of the Mo–support interactions leads to a higher activity. Visser *et al.* have suggested that electronic factors play a role (*52*). Mo–S bonds would be polarised by adjacent Mo–O–Al bonds and breaking of Mo–O–Al bonds would lead to less polarisation and an increase in catalytic activity. Also steric explanations have been proposed. Hayden and Dumesic (*53*), and Ramirez *et al.* (*54*) have suggested from TEM measurements that the $MoS_2$ particles become oriented at an angle to the support when Mo–support interactions are broken. The reactants would have better access to the active site on the $MoS_2$ edge, which would result in an increase in the catalytic activity. However, in principle also the opposite hypothesis could be defended: When strong Mo–support bonds are present the $MoS_2$ particles are standing up; one side of the $MoS_2$ slabs is bonded to the support and the Co sites on this side are not accessible. When the Mo–support bonds are broken, the particle might lie flat on the support and all active sites could participate in the catalysis. Several authors have mentioned that stacking of $MoS_2$ slabs occurs when Mo–O–Al bonds are broken (*10*, *55*, *56*). After stacking there would be less steric hindrance for the reactants. Recently Daage and Chianelli suggested instead that stacking decreases the activity, because Mo atoms at the edges of the second and further $MoS_2$ sheets have a lower activity than those at the edges of the top $MoS_2$ sheet (*57*). Whatever is the case, stacking cannot explain the passivation effect in our catalysts, since the TEM results unambiguously show that no change in stacking occurs for the Co–Mo(0.3)/$Al_2O_3$ catalyst.

As to the mechanism by which Mo–support interactions are broken, several possibilities can be considered. First, it is likely that sulfate is formed during the oxidation of the $MoS_2$ particles (*23*). Sulfate could act as a modifier in the same way as phosphate, which has been shown to decrease Mo–support interactions (*3*, *58*, *59*), thereby increasing the catalytic activity of the CoMoS structure (*4*, *6*). Sulfate can, indeed, change the surface properties of $Al_2O_3$. For instance, the binding energy of $H_2S$ on $Al_2O_3$ changed when $SO_4^{2-}$ was added to the support (*60*). Another way of breaking Mo-support interactions is by Co-promoted sulfidation. Co atoms may move around the $MoS_2$ edges during a passivation–sulfidation cycle, either by leaving the edges during passivation and returning to them during resulfidation, or by changing their position on the edge during passivation. In this way they could migrate toward the Mo–O–Al linkages and help in their sulfidation during the resulfidation step. It has been observed that Ni strongly enhances the sulfidation of W in Ni–W/$Al_2O_3$ catalysts (*61*). Co could, in a similar way, enhance the sulfidation of Mo, and after each passivation–resulfidation cycle more and more Mo–support bonds would be broken, causing an increase in the catalytic activity. The influence of the passivation time can be explained in the same way. The longer the passivation treatment, the more Co atoms are oxidized, and the more Mo–O–Al bonds can be sulfided. On the other hand, a single passivation of one week has less effect than seven passivations of 1 night. This may be due to the heating which will undoubtedly take place during the initial phase of a passivation. The resulting temperature increase will promote oxidation of the sulfidic catalyst and as a consequence the larger the number of passivation cycles, the more exothermicity will play a role.

### *Influence of Co/Mo Atomic Ratio and Passivation Temperature*

The results in Figs. 3 and 4 and Table 2 show that the effect of passivation on the catalytic activity depends on the Co/Mo ratio. At low and high Co/Mo ratios the effect is small and at an intermediate ratio there is a maximum, which is dependent on the number of passivation cycles applied (Fig. 4). The larger the number of passivation cycles, the more the maximum shifts to a lower Co/Mo ratio. Passivation and resulfidation probably cause the $MoS_2$ particles to sinter, and to drive Co off the $MoS_2$ edge at high Co/Mo ratios, because not enough edge is present to accommodate all Co atoms. In this way, the increase in activity caused by the decrease in Mo–support interactions is compensated by a decrease in the amount of CoMoS structure. At low Co/Mo ratios all Co can still be accommodated on the $MoS_2$ edge and is present as CoMoS structure, thus enabling a maximum increase in catalytic activity, while at high Co/Mo ratios $Co_9S_8$ formation lowers the activity. However, the TEM and Mo EXAFS results do not show a strong sintering. The reason for this may be that the crystallites seen by TEM are not single crystalline, but are conglomerates of small single crystals, or that the $MoS_2$ particles contain many dislocations and fault lines. This would explain why the Mo–Mo coordination number determined by EXAFS leads to a much smaller estimate (9 Å) of the $MoS_2$ crystal size than the slab size of 30 Å determined by TEM. EXAFS measures the size of the single-crystalline domains, whereas TEM observes an overall size. If this were the case, after catalyst preparation the Co atoms would also be located at the edges and fault lines inside the overall $MoS_2$ structures, where they would be inaccessible for reactants. Passivation–resulfidation cycles may heal the small domains together and the Co atoms would be forced to go to the edges on the exterior of the overall $MoS_2$ structures. In this way they would become available for catalysis, which would explain the increased activity by passivation at low Co/Mo ratios.

Figure 6 shows that the activity increase for the Co–Mo(0.3)/$Al_2O_3$ catalyst goes through a maximum when the passivation temperature is around 340 K. Apparently, a higher passivation temperature accelerates the oxidation process, leading to a larger activity increase. When the passivation temperature is too high, however, part of the Mo atoms might form new Mo–O–Al bonds, and Co atoms may diffuse into the $Al_2O_3$ support and be lost for promotion. Even after a passivation at 673 K during one night a positive effect on the activity was observed. This is unexpected, since at such a high temperature the Mo should be completely oxidized (*62*), and a large number of new Mo–O–Al bonds might have been formed. Yoshimura *et al.* have suggested that in a Co-promoted catalyst exposure to air leads to the formation of $CoSO_4$, which protects the $MoS_2$ from further oxidation (*63*). Since oxidation of $MoS_2$ takes place from the edges inward (*64*), the bulk of the $MoS_2$ particles would in this way not be oxidized. Göbölös *et al.* also observed that a promoted catalyst is much less sensitive to air exposure than an unpromoted one (*65*, *66*). Thus, in the Co–Mo(0.3)/$Al_2O_3$ catalyst the $MoS_2$ might only be partly oxidized without the formation of many Mo–O–Al bonds. This would explain why even at high passivation temperatures a positive effect on the activity is seen.

### *The Ni–Mo Catalysts*

The Ni–Mo catalysts (Ni–Mo/$Al_2O_3$, Ni–Mo(NTA)/$Al_2O_3$, and Ni–Mo/C(Norit)) show essentially the same behavior as their Co–Mo analogues, albeit that more passivation cycles and longer passivation times per cycle are necessary to obtain the same activity increase. This can probably be explained by the well-known higher kinetic stability of $Ni^{2+}$ compared to $Co^{2+}$ (*67*), causing the breaking and remaking of Ni–ligand bonds in the Ni–Mo catalyst to proceed more slowly than that of Co–ligand bonds in the Co–Mo catalysts. As a consequence, Ni–Mo catalysts need longer passivation times than Co–Mo catalysts for similar activity increases. The final activity increase (i.e., after the last passivation) is larger for the Ni–Mo catalysts than that for the Co–Mo catalysts. This might be due to a lower effectiveness of Ni for sulfiding Mo–O–Al bonds. Due to a lower effectiveness more Mo–support interactions would be present after the first sulfidation (the S catalyst) in the case of Ni and the maximum increase in activity that could be obtained for Ni–Mo catalysts would be higher than for Co–Mo catalysts.

## CONCLUSIONS

By exposing a sulfided Co–Mo/$Al_2O_3$ catalyst to ambient air at room temperature (passivation) and to a subsequent resulfidation, improvements in the catalytic activity of this catalyst for thiophene hydrodesulfurization up to 260% can be obtained. This activity increase is connected with the influence that oxygen has on the catalyst. Co EXAFS, XANES, and MES measurements prove that the environment of the Co atoms does not change, indicating that the active sites before and after passivation are the same. Passivation and resulfidation only cause minor changes in the activity of the Co–Mo(NTA)/$Al_2O_3$, Co–Mo/$TiO_2$, Co–Mo/C(Lonza), and Co–Mo/C(Norit) catalysts, which suggests that a change in the Mo–support interactions is responsible for the activity increase of the Co–Mo/$Al_2O_3$ catalyst. These Mo–support interactions are broken during the passivation and resulfidation, causing an increase in the catalytic activity. The increase in the Mo–S coordination number after a passivation–resulfidation treatment documents this conclusion. The Co EXAFS shows that in the passivated catalyst the Co–Mo coordination number is strongly decreased. The Co atoms become detached from the $MoS_2$ edge, and, after sulfidation, can migrate to a different Mo site on the $MoS_2$ edge. In this way Co atoms can move toward Mo–O–Al linkages and help in the sulfidation of these linkages, thus breaking Mo–support interactions.

The activity increase by passivation is lowest at high Co/Mo atomic ratios, while at an atomic ratio of 1.0 even a decrease in activity is seen. These findings can be explained in several ways. First, although the TEM results do not show any sign of sintering of $MoS_2$ in the Co–Mo(0.3)/$Al_2O_3$ catalyst, it is possible that sintering occurs at higher Co/Mo ratios. Some Co atoms would be driven off the $MoS_2$ edge, and the positive effect on the activity of a breaking of Mo–support interactions would be counteracted by the negative effect of a decrease in the amount of CoMoS. A second explanation is that at high Co/Mo ratios most Mo–support interactions are already broken during the first sulfidation, in contrast to catalysts with low Co/Mo ratios, where most of these interactions are still intact. The maximum positive effect of passivation is then lower for catalysts with high Co/Mo ratios.

The positive effect of passivation on the activity is highest at a passivation temperature of 340 K. Raising the passivation temperature above room temperature apparently causes a more extensive oxidation of Co, which leads to a more extensive breaking of Mo–O–Al bonds, and to a larger activity increase. When the passivation temperature is too high, however, new Mo–O–Al bonds are formed, and part of the positive effect of passivation is lost.

Experiments on the Ni–Mo/$Al_2O_3$, Ni–Mo(NTA)/$Al_2O_3$, and the Ni–Mo/C(Norit) catalysts show that Ni–Mo catalysts behave in the same way as their Co–Mo counterparts.

## ACKNOWLEDGMENTS

We thank Prof. Dr. D. C. Koningsberger and coworkers from The Eindhoven University of Technology, The Netherlands, for their help with the EXAFS measurements.

## REFERENCES

1. Muralidhar, G., Massoth, F. E., and Shabtai, J., *J. Catal.* **85,** 44 (1984).
2. Ramirez de Agudelo, M. M., and Morales, A., *in* "Proceedings, 9th International Congress on Catalysis, Calgary, 1988" (M. Ternan and M. J. Phillips, Eds.), p. 42. Chem. Institute of Canada, Ottawa, 1988.
3. Fierro, J. L. G., López Agudo, A., Esquivel, N., and López Cordero, R., *Appl. Catal.* **48,** 353 (1989).
4. Eijsbouts, S., van Gestel, J. N. M., van Veen, J. A. R., de Beer, V. H. J., and Prins, R., *J. Catal.* **131,** 412 (1991).
5. van Veen, J. A. R., Gerkema, E., van der Kraan, A. M., and Knoester, A., *J. Chem. Soc. Chem. Commun.*, 1684 (1987).
6. van Veen, J. A. R., Gerkema, E., van der Kraan, A. M., Hendriks, P. A. J. M., and Beens, H., *J. Catal.* **133,** 112 (1992).
7. Scheffer, B., van Oers, E. M., Arnoldy, P., de Beer, V. H. J., and Moulijn, J. A., *Appl. Catal.* **25,** 303 (1986).
8. Arteaga, A., Fierro, J. L. G., Grange, P., and Delmon, B., *Appl. Catal.* **34,** 89 (1987).
9. Candia, R., Topsøe, H., and Clausen, B. S., *in* "Proceedings 9th Iberoamerican Symposium on Catalysis, Lisbon, 1984," p. 211.
10. Candia, R., Sørensen, O., Villadsen, J., Topsøe, N.-Y., Clausen, B. S., and Topsøe, H., *Bull. Soc. Chim. Belg.* **93,** 763 (1984).
11. Miciukiewicz, J., and Massoth, F. E., *J. Catal.* **119,** 531 (1989).
12. Kolboe, S., and Amberg, C. H., *Can. J. Chem.* **44,** 2623 (1966).
13. de Beer, V. H. J., Bevelander, C., van Sint Fiet, T. H. M., Werter, P. G. A. J., and Amberg, C. H., *J. Catal.* **43,** 68 (1976).
14. Massoth, F. E., Kim, C.-S., and Cui, J.-W., *Appl. Catal.* **58,** 199 (1990).
15. Browne, V. M., Louwers, S. P. A., and Prins, R., *Catal. Today* **10,** 345 (1991).
16. Louwers, S. P. A., and Prins, R., *J. Catal.* **133,** 94 (1992).
17. Bouwens, S. M. A. M., Koningsberger, D. C., de Beer, V. H. J., and Prins, R., *J. Phys. Chem.* **95,** 123 (1991).
18. Bouwens, S. M. A. M., Prins, R., de Beer, V. H. J., and Koningsberger, D. C., *J. Phys. Chem.* **94,** 3711 (1990).
19. Sasaki, S., Fujino, K., Takeuchi, Y., *Proc. Jpn. Acad.* **55,** 43 (1979).
20. van der Kraan, A. M., and Niemantsverdriet, J. W., *in* "Industrial Applications of the Mössbauer Effect" (G. J. Long and J. G. Stevens, Eds.), p. 609. Plenum, New York, 1986.
21. Crajé, M. W. J., de Beer, V. H. J., and van der Kraan, A. M., *Bull. Soc. Chim. Belg.* **100,** 953 (1991).
22. Clausen, B. S., Mørup, S., Topsøe, H., and Candia, R., *J. Physique* **37,** C6-249 (1976).
23. Brinen, J. S., and Amstrong, W. D., *J. Catal.* **54,** 57 (1978).
24. Clausen, B. S., Lengeler, B., Candia, R., Als-Nielsen, J., and Topsøe, H., *Bull. Soc. Chim. Belg.* **90,** 1249 (1981).
25. Lytle, F. W., Wei, P. S. P., Greegor, R. B., Via, G. H., and Sinfelt, J. H., *J. Chem. Phys.***70,** 4849 (1979).
26. Zmierczak, W., MuraliDhar, G., and Massoth, F. E., *J. Catal.* **77,** 432 (1982).
27. Bodrero, T. A., and Bartholomew, C. H., *J. Catal.* **84,** 145 (1983).
28. Parham, T. G., and Merrill, R. P., *J. Catal.*, **85,** 295 (1984).
29. Schrader, G. L., and Cheng, C. P., *J. Catal.* **80,** 369 (1983).
30. Schrader, G. L., and Cheng, C. P., *J. Catal.* **85,** 488 (1984).
31. Eisenberger, P., and Brown, G. S., *Solid State Commun.* **29,** 481 (1979).
32. Chiu, N.-S., Bauer, S. H., and Johnson, M. F. L., *J. Catal.* **89,** 226 (1984).
33. Kisfaludi, G., Leyrer, J., Knözinger, H., and Prins, R., *J. Catal.* **130,** 192 (1991).
34. Chiu, N.-S., Bauer, S. H., and Johnson, M. F. L., *J. Catal.* **98,** 32 (1986).

35. Topsøe, H., Candia, R. Topsøe, N.-Y., and Clausen, B. S., *Bull. Soc. Chim. Belg.* **93,** 783 (1984).
36. Crajé, M. W. J., Gerkema, E., de Beer, V. H. J., and van der Kraan, A. M., *Hyperfine Interact.* **57,** 1795 (1990).
37. Chianelli, R. R., Pecoraro, T. A., Halbert, T. R., Pan W.-H., and Stiefel, E. I., *J. Catal.* **86,** 226 (1984).
38. de Beer, V. H. J., Duchet, J. C. and Prins, R., *J. Catal.* **72,** 369 (1981).
39. Vissers, J. P. R., de Beer, V. H. J., and Prins, R., *J. Chem. Soc., Faraday Trans. 1* **83,** 2145 (1987).
40. Moon, S., and Ihm, S., *Appl. Catal.* **42,** 307 (1988).
41. Hayden, T. F., Dumesic, J. A., Sherwood, R. D., and Baker, R. T. K., *J. Catal.* **105,** 299 (1987).
42. Scheffer, B., Arnoldy, P., and Moulijn, J. A., *J. Catal.* **112,** 516 (1988).
43. Meyer, F. J., Erich Pietsch, E. H., and Kotowski, A., *in* "Gmelins Handbuch der Anorganische Chemie, Kohlenstoff" (A. Kotowski, Ed.), Part B, p. 917. Verlag Chemie, Weinheim, 1968.
44. van Driel, J., *in* "Activated Carbon . . . a Fascinating Material" (A. Capelle and F. de Vooys, Eds.), p. 40. Norit, Amersfoort, 1983.
45. Massoth, F. E., *Adv. Catal.* **27,** 265 (1978).
46. Topsøe, H., Clausen, B. S., Burriesci, N., Candia, R., and Mørup, S., *Stud. Surf. Sci.* **3,** 479 (1979).
47. Ng, K. Y. S., and Gulari, E., *J. Catal.* **95,** 33 (1985).
48. Duchet, J., van Oers, E. M., Arnoldy, P., de Beer, V. H. J., and Moulijn, J. A., *Appl. Catal.* **25,** 303 (1986).
49. Shimada, H., Sato, T., Yoshimura, Y., and Nishijima, A., *J. Catal.* **110,** 275 (1988).
50. Okamoto, Y., Maezawa, A., and Imanaka, T., *J. Catal.* **120,** 29 (1989).
51. Pratt, K. C., Sanders, J. V., and Christov, V., *J. Catal.* **124,** 416 (1990).
52. Vissers, J. P. R., Scheffer, B., de Beer, V. H. J., Moulijn, J. A., and Prins, R., *J. Catal.* **105,** 277 (1987).
53. Hayden, T. F., and Dumesic, J. A., *J. Catal.* **103,** 366 (1987).
54. Ramirez, J., Fuentes, S., Diaz, G., Vrinat, M., Breysse, M., and Lacroix, M., *Appl. Catal.* **52,** 211 (1989).
55. Beuken, J.-M., and Bertrand, P., *Surf. Sci.* **162,** 329 (1985).
56. Kemp, R. A., Ryan, R. C., and Smegal, J. A., *in* "Proceedings 9th International Congress on Catalysis, Calgary, 1988" (M. Ternan and M. J. Phillips, Eds.), p. 128. Chem. Institute of Canada, Ottawa, 1988.
57. Daage, M., Chianelli, R. R., and Ruppert, A. F., *in* "New Frontiers in Catalysis, 10th Int. Congress on Catalysis" (L. Guczi, F. Solymosi and P. Tétényi, Eds.), p. 571. Akadémiai Kiadó, Budapest, 1993.
58. Gishti, K., Iannibello, A., Marengo, S., Morelli, G., and Tittarelli, P., *Appl. Catal.* **12,** 381 (1984).
59. van Veen, J. A. R., Hendriks, P. A. J. M., Andréa, R. R., Romers, E. J. G. M., and Wilson, A. E., *J. Phys. Chem.* **94,** 5282 (1990).
60. Okamoto, Y., Oh-Hara, M., Maezawa, A., Imanaka, T., and Teranishi, S., *J. Phys. Chem.* **90,** 2396 (1986).
61. Scheffer, B., Mangnus, P. J., and Moulijn, J. A., *J. Catal.* **121,** 18 (1990).
62. Grove, C. L., and Schmidt, L. D., *Appl. Surf. Sci.* **35,** 199 (1988–1989).
63. Yoshimura, Y., Matsubayashi, N., Yokokawa, H., Sato, T., Shimada, H., and Nishijima, A., *Ind. Eng. Chem. Res.* **30,** 1092 (1991).
64. Roxlo, C. B., Daage, M., Leta, D. P., Liang, K. S., Rice, S., Ruppert, A. F., and Chianelli, R. R., *Solid State Ionics* **22,** 97 (1986).
65. Göbölös, S., Wu, Q., Andé, O., Delannay, F., and Delmon, B., *J. Chem. Soc. Faraday Trans. 1* **82,** 2423 (1986).
66. Göbölös, S., Wu, Q., Delannay, F., Grange, P., and Delmon, B., *Polyhedron* **5,** 219 (1986).
67. Sykes, A. G., *in* "Kinetics of Inorganic Reactions," p. 246. Pergamon, Oxford, 1966.